Interactions between rare-gas atoms: an effective medium study

M J Puska and R M Nieminen

Laboratory of Physics, Helsinki University of Technology, 02150 Espoo, Finland

Abstract. The interactions between rare-gas atoms are studied using the effective medium theory developed by Jacobsen *et al*. This theory is based on solving the interaction of a single atom with homogeneous electron gas. First the necessary electron structure calculations are performed by employing the density functional formalism within the local-density approximation (LDA) for electron exchange and correlation effects. The binding properties of the rare-gas atoms are then extracted along the lines of the effective medium theory, which previously has been shown to give a good description of simple metals. The results now obtained for rare-gases support these ideas and widen their area of applicability. The cohesive energies and Wigner–Seitz radii obtained for solid Ne, Ar and Kr are in good agreement with experimental values. The present values for the bulk moduli are too large reflecting the inability of the LDA to describe the long-range van der Waals interactions. According to the present model He atoms do not form bound systems. Using a simple nearest-neighbour model the bulk cohesive properties are converted into pair potentials. In the case of Ne, Ar and Kr the pair potentials obtained are in good agreement with previous theoretical and semi-empirical models from the bottom of the attractive well to the highly repulsive region. However, the pair potentials are short-ranged instead of having an $1/R^6$-tail due to the LDA.

1. Introduction

The conventional way to describe the interaction between two rare-gas atoms is to decompose it into two: a repulsive part due to Pauli orthogonalization; and an attractive part, which is the van der Waals interaction arising from the instantaneous charge fluctuations. For practical purposes this picture is often modelled by the Lennard–Jones 6–12 pair potential, in which the increase in the repulsive part is proportional to $1/R^{12}$ when the internuclear distance R decreases and the decay in the attractive part is proportional to $-1/R^6$ when the atoms separate from each other. The pair-potential model can then be successfully applied to obtain the cohesive properties of rare-gas solids. This method is, however, a semi-empirical one, because the parameters of the Lennard–Jones potential are fitted to experimental data.

Of the first-principles methods for calculating rare-gas interactions the configuration interaction (CI) calculation is perhaps the most accurate, but it becomes extremely costly when the number of electrons in the system increases. Hartree–Fock calculations, which do not include the correlation effects, lead to purely repulsive interactions. The work by Gordon and Kim [1] showed that the incorporation of the

correlation effects enables a surprisingly accurate description of the depth and position of the attractive well within an already very simple model. Gordon and Kim constructed the electron densities for dimers non-self-consistently by superimposing free atom densities, and calculated the total energy change, when two free atoms form a dimer, by using *local* approximations for the kinetic energy (the Thomas–Fermi model) and the exchange-correlation energy. Recently, Harris [2] and, independently, Foulkes and Haydock [3] have shown that the Gordon–Kim model can be obtained as an approximate total energy functional in the density-functional theory. They also showed how the local kinetic energy functional can be improved. However, for the rare-gases Harris [2] and Foulkes and Haydock [3] only gave results for He. A comment related to the success of the Gordon–Kim model has been presented by Lang [4], who obtained, within the local-density approximation (LDA), quantitatively good results for the physisorption of rare-gas atoms on jellium surfaces.

In this work we introduce a completely new viewpoint to describe and understand the interactions between rare-gas atoms. Our description is based on the interaction of the rare-gas atom with a homogeneous electron gas consisting of a rigid, positive and constant background charge and a neutralizing, relaxable electron density. The homogeneous electron gas provides the electrons which in the real, condensed rare-gas system are the bound electrons of the neighbouring atoms. Increasing the homogeneous background density mimics the decrease in the distances between the rare-gas atoms when the atomic density is increased. In the electron gas picture the penetration of the electrons inside the electron cloud of the rare-gas atom results, for low background densities, in an *attractive* interaction due to the Coulomb and exchange-correlation energy contributions. (The Coulomb interaction between the positive background charge and the total atom-induced charge is subtracted, because in the real system the positive charge only consists of nuclei.) When the background density increases the interaction becomes increasingly repulsive because the kinetic energy of the system rises rapidly as more and more electron gas states have to be orthogonal against the bound states at the rare-gas atom.

2. Theory

We have solved the electron structure for an atom in the homogeneous electron gas by using the density-functional method within the LDA [5] (we use a local exchange-correlation functional based on the results from Ceperley and Alder [6] and the parameterized form given by Perdew and Zunger [6].) In order to increase the numerical stability when calculating small total energy differences, corresponding to low electron gas densities, we have employed the frozen core approximation. We allow only the uppermost s- and p-orbitals to relax from those of the free atoms. At high electron gas densities it also becomes important to allow the core electron states to relax and therefore we have not made the frozen core approximation when the density parameter r_s is smaller than approximately 4 a_0, (the background electron density $\bar{n} = 1/(4\pi r_s^3/3)$). In the present work the r_s values range from 0.33 a_0 in the very high background density region to 11 a_0 at very low densities.

The link between the solution of the model system (atom in jellium) and the interactions in many-atom systems is the effective medium theory (EMT) [7]. It is an approximate method for calculating the total energy of a system of interacting atoms. The EMT has been used in various applications for describing real systems

with low symmetry, including interatomic forces for molecular dynamics simulations (for reviews see [8]). In addition to the practical applications, the atom-in-jellium/EMT model has proven very useful in systematic studies of the binding properties of atoms, in particular the manner in which these properties are affected by approximations in the exchange-correlation energy functional (e.g. the LDA) [9].
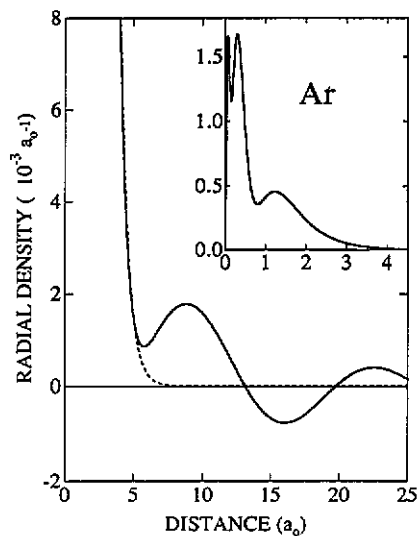

Figure 1. The induced radial electron density $(4\pi r^2 \Delta n(r))$ of an Ar atom in a homogeneous electron gas with $r_s = 7\ a_0$ (full line) compared with the free-atom density (broken line).
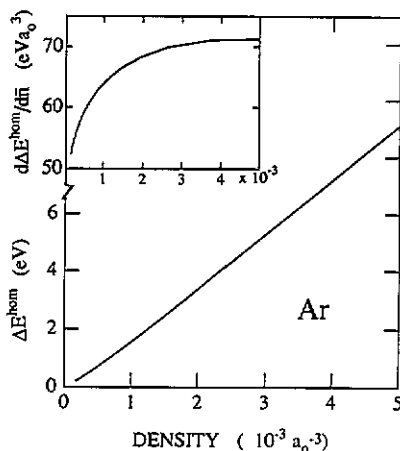
Figure 2. Immersion energy ΔE^{hom} as a function of electron gas density for Ar. The behaviour of the slope of ΔE^{hom} calculated by equation (9) is given in the inset.

The basic ansatz in the EMT [7] is that the electron density $n(r)$ of a many-atom system can be constructed as the superposition of the induced electron densities $\Delta n(r)$ similar to that shown in figure 1 for Ar. Thus,

$$n(r) = \sum_{R_i} \Delta n(|r - R_i|) \qquad (1)$$

where the summation runs over the atomic positions R_i. By making this assumption it is possible to derive an approximate formula for the total energy of the many-atom system in terms of the functions and parameters calculated for the atoms in the homogeneous electron gas. The central concept in the EMT is the cohesive function E_c. It is a function of the background electron density $\bar n$ and is defined as

$$E_c(\bar n) = \Delta E^{\text{hom}}(\bar n) - \alpha(\bar n)\bar n. \qquad (2)$$

Above, $\Delta E^{\text{hom}}(\bar n)$ is the energy required to bring a free atom from vacuum into jellium with density $\bar n$ [5]. It is calculated as a total energy difference. The function α is calculated as

$$\alpha(\bar n) = \int_0^{s(\bar n)} dr\, 4\pi r^2 \phi(r) \qquad (3)$$

where $\phi(r)$ is the induced Coulomb potential

$$\phi(r) = \frac{Z}{r} - \int_0^{s(\bar{n})} \mathrm{d}r \, 4\pi r^2 \frac{\Delta n(r')}{|r - r'|}. \tag{4}$$

In equation (3) the upper limit $s(\bar{n})$ of the integration is the so-called neutral sphere radius, defined by requiring that the total electron density $n(r)$ inside this sphere neutralizes the nuclear charge Z (but not the positive background charge). Thus,

$$\int_0^{s(\bar{n})} n(r) 4\pi r^2 \, \mathrm{d}r = Z. \tag{5}$$

This definition leads to a unique dependence between the radius s and the background density $\bar{n}$. The last term in equation (2) cancels the Coulomb interaction of the positive background charge with the total induced charge density (nucleus + electrons) inside the neutral sphere. Alternatively, in the real system this term can be considered as an attractive electrostatic interaction energy of the atom in a given sphere and the electron density tails from the neighbouring atoms sticking into this sphere.

The experience with the EMT shows that the cohesive function $E_c(\bar{n})$ and the neutral sphere radius $s(\bar{n})$ quite accurately predict the cohesive properties of simple sp-bonded FCC metals [7, 9]. If one eliminates the background density $\bar{n}$ one obtains the usual cohesive energy against atomic volume representation. The minimum values of $E_c(\bar{n})$ and the corresponding $s(\bar{n})$ give the equilibrium cohesive energy and the Wigner–Seitz radius, respectively. Furthermore, the bulk modulus is obtained as

$$B = \frac{1}{12\pi s_0} \frac{\mathrm{d}^2 E_c}{\mathrm{d}s^2}. \tag{6}$$

Later we demonstrate that this simplest form of the EMT also gives a good description of the rare-gas solids, whose band structures represent good insulators with narrow bands. Moreover, the EMT gives a good description of the interaction potential between two rare-gas atoms.

There are numerous experimental and theoretical studies of the interaction potential between two rare-gas atoms as a function of the interatomic distance [10]. These data are also very valuable for our purposes, because they make comparisons possible in a wide range of the interaction from the highly repulsive region to the region beyond the attractive minimum, while the comparison for the bulk cohesive properties gives information only near the minimum. In order to calculate the pair potential from the EMT data we proceed as follows. Because the simplest version of the EMT previously described assumes that the atoms form a perfect FCC lattice [7], the interaction potential in a nearest-neighbour model is one-sixth of the total energy of the lattice per atom. Thus, the pair potential is

$$V(R) = E_c(\bar{n})/6 \tag{7}$$

where the distance R is calculated from the neutral sphere radius corresponding to the same background density $\bar{n}$ (FCC lattice)

$$R = \frac{1}{\sqrt{2}} \left(\frac{16\pi}{3} \right)^{1/3} s(\bar{n}). \tag{8}$$

These equations are the simplest way of constructing the pair potential. The omission of contributions other than the nearest-neighbour contributions is not a severe simplification because the interaction has a short range. The relatively largest effect is near the minimum of the pair potential, where the inclusion of more distant neighbours would raise the potential. For example, in the case of Ar we estimate that the inclusion of the second-nearest neighbours would decrease the depth of the minimum by about 3%.

3. Results and discussion

As an example of the electron density changes when a rare-gas atom is embedded in electron gas, figure 1 shows the induced electron density around an Ar nucleus. The electron gas density parameter r_s has the value of 7 a_0, which corresponds approximately to the minimum of the E_c function. The induced density is compared with the free atom electron density. The densities coincide near the nucleus approximately up to the distance of 5 a_0. This reflects the very compact nature of the rare-gas electron structure also in electron gas. Beyond approximately 5 a_0 the induced density shows Friedel oscillations. First there is a positive oscillation leading to the overscreening of the Ar nucleus.

The $\Delta E^{\text{hom}}(\bar{n})$ curves for He, Ne and Ar have been published in [5] and [11]. Figure 2 shows $\Delta E^{\text{hom}}(\bar{n})$ for Ar in the low background density region, which is now treated in more detail than in our previous work [5]. The results extend to low density with r_s equal to 11 a_0. The results for the other rare-gases are similar. It can be seen that the $\Delta E^{\text{hom}}(\bar{n})$ curve rises nearly linearly from the origin when the background electron density $\bar{n}$ increases. The rise is due to the increase in the kinetic energy, and signals that the interaction between a rare-gas atom and the homogeneous electron gas is repulsive. The rise of the $\Delta E^{\text{hom}}(\bar{n})$ curves is not exactly linear as stated earlier [5, 11]. We find that for all rare-gases the second derivative of $\Delta E^{\text{hom}}(\bar{n})$ is positive near the origin. As a matter of fact, the first derivative can be obtained directly by integrating directly the induced Coulomb potential $\phi(r)$ [12]

$$\frac{\mathrm{d}\Delta E^{\text{hom}}}{\mathrm{d}\bar{n}} = \int_0^\infty \mathrm{d}r\, 4\pi r^2 \phi(r). \qquad (9)$$

The behaviour of the derivative calculated from this equation is shown for Ar in the inset of figure 2. The derivative is seen to decrease rapidly at low densities in agreement with the behaviour of the $\Delta E^{\text{hom}}(\bar{n})$ curve.

The $E_c(\bar{n})$ functions are given for the rare-gases from He to Kr in figure 3. The curves are continued at low densities down to values ($r_s \approx 11$) for which we were still able to find stable results. In the case of Ne, Ar and Kr there is a negative minimum at low densities corresponding approximately to the r_s value of 7–8 a_0. In the case of He we do not find a minimum, but the $E_c(\bar{n})$ curve rises monotonically from the lowest densities treated. The existence of the minimum signals an attractive interaction between the rare-gas atoms. Figure 4, in which the $E_c(\bar{n})$ curve for Ne is decomposed into the various components of the energy change in the embedding process, shows that the negative minimum results from a very delicate overcancellation of the repulsive kinetic contribution by the attractive Coulomb and exchange-correlation parts. When the background electron density increases, the positive curvature of the kinetic energy becomes increasingly dominant and the interaction becomes repulsive.
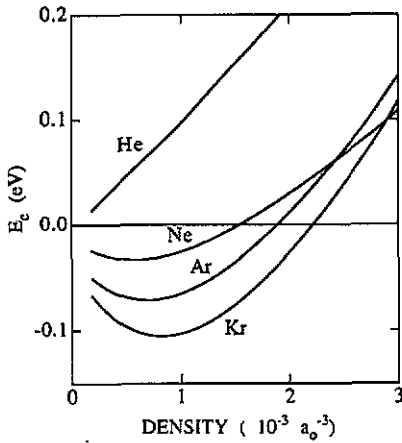
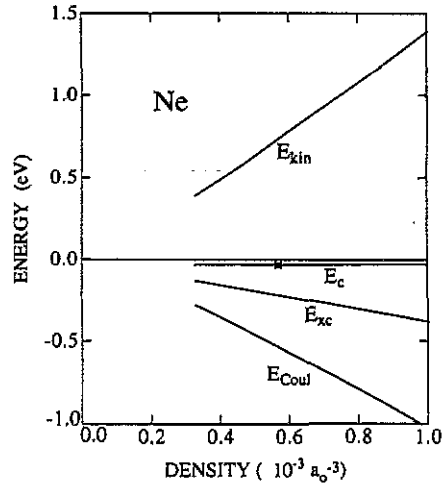**Figure 3.** Cohesive function E_c (equation (2)) as a function of electron gas density for He, Ne, Ar and Kr.

Figure 4. Decomposition of the cohesive function E_c for Ne into kinetic (E_{kin}), exchange-correlation (E_{xc}) and Coulomb (E_{Coul}) parts near the minimum (x) of $E_c(\bar{n})$. E_{kin}, E_{xc} and E_{Coul} are defined as the changes of the values of the corresponding energy functionals when a free atom is embedded in a homogeneous electron gas [5]. The Coulomb part contains also the term $-\alpha(\bar{n})\bar{n}$ defined in equation (2).

The cohesive properties calculated for the FCC rare-gas solids Ne, Ar and Kr are compared with the experimental ones in figure 5 [13]. In the case of Ne the theory leads to overbinding: the theoretical cohesive energy is about 1.7 times the experimental one. For Ar and Kr the agreement is better, the theoretical values being about 10% below the experimental one. However, if one takes the relative smallness of the Ne cohesive energy into account, it can be concluded that the overall experimental trend is fairly well reproduced in the calculations. The theoretical values for the Wigner–Seitz radii are consistently less than the measured ones, but the disagreement is only 3–5%. The underestimation of the Wigner–Seitz radii means that the effective interactions between two rare-gas atoms have too short a range in the present model. The effects due to the omission of the zero-point motion are in the same direction but smaller. On the other hand, the close agreement shows that the electron cloud around the nucleus (in the sense of the neutral sphere) is surprisingly well described by the atom-in-jellium model. The bottom part of figure 5 compares the theoretical and experimental bulk moduli. The theoretical values are too high reflecting the fact that the curvature of the $E_c(\bar{n})$ near the minimum is too large. The large curvature arises from the low density side of the minimum: the $E_c(\bar{n})$ curve rises too quickly as the electron density decreases. This means that the present model based on the LDA gives too short a range for the interaction between the atoms. In the effective pair-potential discussed later this short-range nature appears even more clearly.

The well-known deficit of the LDA (for a recent review, see [14]) [9] is to overbind diatomic molecules and bulk solids. The overbinding is largest when the atomic p- or d-shell is partially filled. The overbinding decreases strongly towards smaller occupation
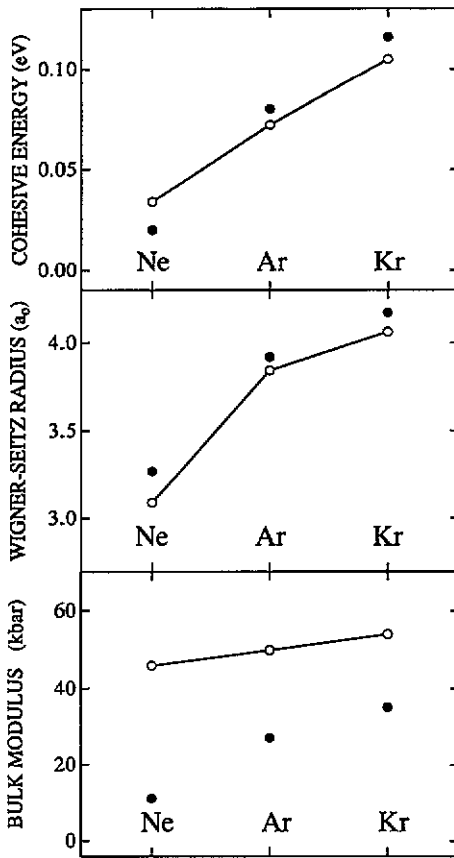
Figure 5. Cohesive properties of solid Ne, Ar and Kr calculated in the EMT (open circles) in comparison with the experimental values [13] (black circles).

of these shells and also near the completion of the partially filled shell. The binding energies as well as the LDA overbinding deficit are of the order of a few eV, thus one or two orders in magnitude larger than the energies which we now consider for rare-gases. For these reasons it is very unlikely that the large LDA overbinding and the overbinding now seen for rare-gases are directly related.

The pair potentials calculated for Ne, Ar and Kr using the EMT and equations (7) and (8) are compared with semi-empirical potentials in figure 6. The agreement is surprisingly good, if one takes into account the approximations in equations (7) and (8) and the fact that our parameter-free model is based on the interaction of a *single* atom with free electron gas. In the case of Ne–Ne interaction our values indicate overbinding in comparison with the semi-empirical curve but for Ar and Kr the minima of the potential curves agree very well with the semi-empirical ones. The bond lengths are, according to our model, systematically smaller than those obtained from the semi-empirical fits. The largest difference is seen in the case of Kr. The slopes of the repulsive walls are in fairly good agreement, especially in the cases of Ne and Ar. At high energies the present values for Ar seem to be somewhat low. However, in these comparisons one should bear in mind that there are significant differences between
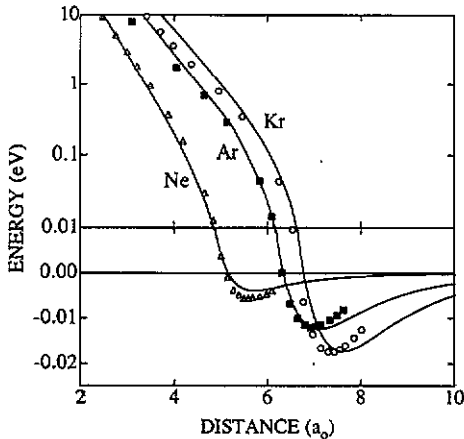
Figure 6. Pair potentials for rare-gases. The present EMT results for Ne (triangles), Ar (black squares), and Kr (circles) are compared with the semi-empirical pair potentials (full lines) taken from Siska *et al*, Aziz and Slaman, and Buck *et al* respectively [15]. Note the change between the logarithmic and linear scales at +0.01 eV.

different semi-empirical pair potentials in the energy range from 1 to 10 eV (for a recent review, see [10]). However, the most important difference between the present results and the semi-empirical curves can be clearly seen from figure 6: the present theoretical curves rise too quickly at large distances. This reflects the fact that the LDA cannot describe the $1/R^6$ van der Waals interaction.

The present results (crosses) for the Ar-Ar potential are compared with previous theoretical calculations in figure 7. The full line denotes recent accurate calculations by McLean *et al* [16] employing the method of interacting correlated fragments (ICF). The broken line is the Gordon–Kim result [1]. The ICF treats the correlation effects non-locally and therefore leads to the correct long-range behaviour. The Gordon–Kim model is based on the LDA and therefore results in a short-range interaction. It is interesting to note that our results approach the Gordon–Kim curve from below when the distance increases. A similar approach also takes place in the case of Ne and Kr.

In the repulsive region just above zero energy the present results and the ICF calculations are in very good agreement. The Gordon–Kim curve lies somewhat below the other two indicating an underestimation of the kinetic energy, when it is also calculated within the LDA (Thomas-Fermi). Another reason, which may lower the Gordon–Kim values is related to the theorem proved by Zaremba [17] for the Harris functional, from which the Gordon–Kim model is an approximation. He showed that the Harris functional has a local maximum at the true self-consistent electron density unless the electronic system possesses anomalous screening properties. It is not, however, possible to draw firm conclusions from figure 7 on this basis, because the different curves are calculated by employing such different approximations.

At the higher repulsive region the Gordon–Kim and the present models give results in close agreement whereas the ICF values lie somewhat higher. The agreement between the present and the Gordon–Kim models at the highest energies is somewhat surprising, because for example around 600 eV about one-third of the repulsive interaction in the Gordon–Kim model comes from Coulomb energy which is at that distance repulsive due to the nucleus–nucleus interaction. In the present model the interaction

between two atoms is calculated via the total energy of a bulk FCC solid formed by neutral spheres, among which there is no repulsive Coulomb interaction. Thus, in the present model, the increase in the kinetic energy substitutes the direct electrostatic interaction. Thus, the present pair-potential construction at high energies serves as an alternative approach to the usual model of a Coulomb repulsion of two screened nuclei (for a recent review, see [18]). The present model underlines the importance of the accurate treatment of the kinetic energy. An additional interesting detail in the repulsive region is that, according to figure 7, both the Gordon–Kim and the present model show a change in the slope (in the logarithmic derivative) of the interaction potential around 30 eV. This change reflects the shell structure of the Ar atom.
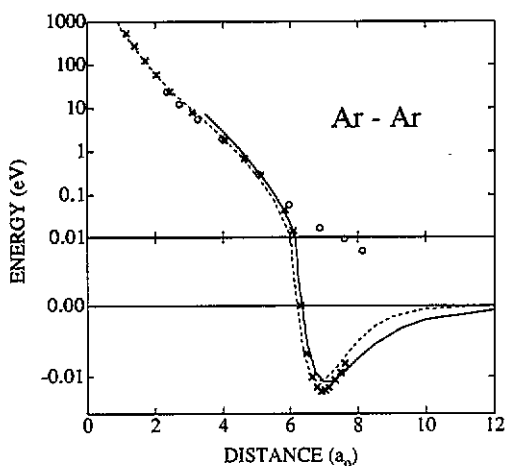

Figure 7. Theoretical Ar–Ar pair potentials. The present EMT potential (crosses) is compared with the result from an ICF calculation (full line) [16] and with the Gordon–Kim potential (broken line) [1]. The present result based on the LMTO-ASA method is also shown (open circles). Note the change between the logarithmic and linear scales at +0.01 eV.

Figure 8. Theoretical He–He pair potentials. The present EMT potential (crosses) is compared with the result from an ICF calculation (full line) [20] and with the Gordon–Kim potential (broken line) [1]. The present result based on the LMTO-ASA method is also shown (open circles). Note the change between the logarithmic and linear scales at +0.01 eV.
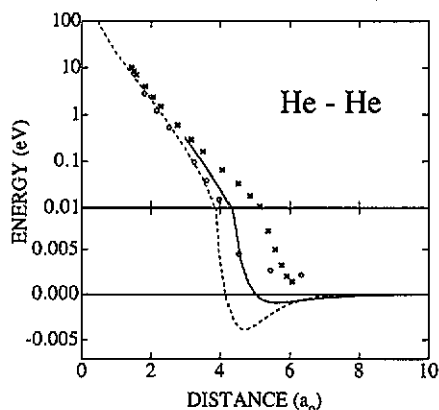
For comparison, we have also determined the Ar–Ar pair potential by calculating the cohesive energy of an FCC Ar-solid by using the linear-muffin-tin-orbital (LMTO) (for a recent review, see [19]) method within the atomic spheres approximation (ASA) for different values of the lattice parameter and then using equations (7) and (8). The results are denoted by the open circles in figure 7. We see that at small distances and high interaction energies the LMTO-ASA results coincide very well with the EMT results and also with the Gordon–Kim results. The common nominator in all these three calulations is the rigid spherical symmetry of the constituent electron structures around the nuclei: In the Gordon–Kim model two spherical atoms overlap but their electron densities are not allowed to relax. In the LMTO-ASA and EMT the electron densities relax, but only so that the spherical symmetry around the nuclei is preserved. In the ICF calculation for the Ar *dimer* there is no such a limitation and this is perhaps the reason why the ICF curve is above the other results at the highest energies for which ICF results exist.

Figure 7 shows that our LMTO-ASA results deviate from the other results at large distances so that the pair interaction shows no minimum at all. We believe that the lack of the attractive minimum is due to the incomplete basis function set. We have used ASA with s, p, d and f partial waves only, but higher angular-momentum components would be required when the sphere radius increases. In our atom-in-jellium calculations we have used partial waves up to $l = 9$, and we have tested that around the attractive minimum waves at least up to $l = 6$ are needed in order to stabilize the results. In order to treat the attractive region more accurately in LMTO one should include the so-called combined correction in the calculation of the total energy [19].

The various theoretical results for the He–He interaction are compared in figure 8. The full line is the ICF result [20] showing a weak minimum at large distances. The Gordon–Kim result [1] (broken curve) is in the repulsive region again below the ICF values and there is much too attractive a minimum. The potential [2] obtained using the Harris functional (not shown) would lie even below the Gordon–Kim results. The present EMT results (crosses) are much too repulsive at large distances and no minimum results. This different behaviour of He compared with the other rare-gases in the present model reflects the very compact electron structure of the small He atom. At smaller distances the EMT values seem to approach the Gordon–Kim potential. The LMTO-ASA results show again no attraction at all, but when going towards the more repulsive region the results essentially coincide with the Gordon–Kim curve, supporting the conclusions made above in the case of Ar.

4. Summary

We have studied the interaction between homonuclear rare-gas atoms in the atom-in-jellium/EMT model. The EMT gives the cohesive properties of FCC solids, and a nearest-neighbour interaction model is used in order to obtain the pairwise potentials between atoms. The calculations predict that Ne, Ar and Kr atoms form bound systems whereas the interactions between He atoms are always repulsive. The interactions have too short a range (no long-range van der Waals interaction), and this deficiency is due to the LDA. As a result of this defect the bulk moduli for solid rare-gases are too large and the pair potentials decay too rapidly. However, the cohesive energies and lattice constants predicted for the solid state are in good agreement with experiments. The same is true also for the pair potentials on the repulsive side of the interaction. An especially interesting result is that the pair potentials calculated essentially coincide with the Gordon–Kim [1] results up to the highly repulsive region of the interaction (in the case of Ar we were able to get stable results up to the dimer energy of about 500 eV). Due to the ASA the repulsion in our EMT calculations originates purely from the kinetic energy, which should be contrasted with the rapid increase in the nucleus–nucleus repulsion in other pair-potential models [1, 18]. The success of the EMT in the highly repulsive region also means that it can be applied, for example, in molecular-dynamics simulations with high-energy atoms. Moreover, this indicates the present model can be used to predict pair-interaction energies around 100 eV. This energy region is of great importance for the scattering of ion beams from solid surfaces.

References

[1]   Gordon R G and Kim Y S 1972 *J. Chem. Phys.* **56** 3122
[2]   Harris J 1985 *Phys. Rev.* B **31** 1770
[3]   Foulkes W M and Haydock R 1989 *Phys. Rev.* B **39** 12520
[4]   Lang N D 1981 *Phys. Rev. Lett.* **46** 842
[5]   Puska M J, Nieminen R M and Manninen M 1981 *Phys. Rev.* B **24** 3037
[6]   Ceperley D M and Alder B J 1980 *Phys. Rev. Lett.* **45** 566
      Perdew J P and Zunger A 1981 *Phys. Rev.* B **23** 5048
[7]   Jacobsen K W, Nørskov J K and Puska M J 1987 *Phys. Rev.* B **35** 7423
[8]   Jacobsen K W 1988 *Comm. Cond. Matter Phys.* **14** 129; 1990 *Many-Atom Interactions in Solids (Springer Proceedings in Physics 48)* ed R M Nieminen, M J Puska and M Manninen (Heidelberg: Springer) p 34
[9]   Puska M J and Nieminen R M 1991 *Phys. Rev.* B at press
[10] Aziz R A 1984 *Inert Gases (Springer Series in Chemical Physics 34)* ed M L Klein (Heidelberg: Springer) p 5
[11] Stott M J and Zaremba E 1982 *Can. J. Phys.* **60** 1145
[12] Stott M J and Zaremba E 1980 *Phys. Rev.* B **22** 1564
[13] Kittel C 1976 *Introduction to Solid State Physics* (New York: Wiley)
[14] Jones R O and Gunnarsson O 1989 *Rev. Mod. Phys.* **61** 689
[15] Siska P E, Parson J M, Schafer T P and Lee Y T 1971 *J. Chem. Phys.* **55** 5762
      Aziz R A and Slaman M J 1989 *J. Chem. Phys.* **92** 1030
      Buck U, Dondi M G, Valbusa U, Klein M L and Scoles G 1973 *Phys. Rev.* A **8** 2409
[16] McLean A D, Liu B and Barker J A 1988 *J. Chem. Phys.* **88** 6339
[17] Zaremba E 1990 *J. Phys.: Condens. Matter* **2** 2479
[18] Ziegler J F, Biersack J P and Littmark U 1985 *The Stopping and Range of Ions in Solids* (New York: Pergamon)
[19] Andersen O K, Jepsen O and Sob M 1987 *Electronic Band Structure and Its Applications* ed M Yussouffy (Heidelberg: Springer) p 1
[20] Liu B and McLean A D 1989 *J. Chem. Phys.* **91** 2348